Journal of the Brazilian Society of Mechanical Sciences and Engineering (2022) 44:132
https://doi.org/10.1007/s40430-022-03438-6

TECHNICAL PAPER

Regression equations of the biodiesel permittivity from its composition, molecular structure, and temperature

Dario Alviso[1,2]

Received: 19 October 2021 / Accepted: 20 February 2022

Abstract
The measurement of electrical permittivity (EP) has been used in many biodiesel (BD) studies. They include the characterization of different oil-based BD and its blends with diesel fuel (DF), its adulteration with vegetable oils (VOs), the estimation of the kinematic viscosity and the BD content in its blends with DF, the evaluation of the purification process efficiency after the reaction of transesterification, and the detection of BD aging and fuel quality control. A few hundreds of VOs have the potential for BD production, and their experimental EP values for most of them are not currently known. The EP of BD as a function of its fatty acid methyl ester content and molecular structure is determined in this work using regression equations. A regression analysis was performed using experimental databases for the EP, which included a total of 43 data points in the range of 20–50 °C. The equations were derived using multiple linear regression analysis and accurately reproduced the BD EP's dependence on the carbon chain length and unsaturation level. When the regression equations' results were compared to available experimental data, they showed a high level of agreement. The EP equations' RMSE values utilizing all of the data were lower than 0.038.

Keywords Biodiesel · Electrical · Permittivity · Regression · Fatty acid methyl ester · Molecular structure

1 Introduction

Transesterification of vegetable oils (VOs) or animal fat with short-chain alcohol is currently being used to produce biodiesel (BD) [1–3]. International standards (such as ASTM D6751 and EN 14214) specify physicochemical parameters that must be within specified limits for BD quality assessment, such as density, viscosity, oxidative stability, flash point, acid number, methanol concentration, and methyl esters content [4–6]. Many of these measurements are time-consuming, necessitate specialist staff, are difficult to adapt to online measurements, and require expensive equipment. Thus, other approaches for characterizing BD (such as electrical) are of interest.

Dielectric spectroscopy investigates the interaction of substances with a time-dependent electric field. It is a fast, easy, and non-destructive measurement approach that can be done using low-cost equipment. It's been used to test food quality and detect moisture [7], characterize BD and VOs [8, 9], blends of alcohol with diesel fuel (DF), and BD [10], and BD precursors, such as soybean VO, alcohols, catalysts, and their mixtures [11]. It was also used to determine the kinematic viscosity of BD/DF blends [12], estimate the BD content in blends with DF [13, 14], detect methanol in BD, and determine the efficiency of the purification process after transesterification [15], detect BD aging and fuel quality control [16, 17], and study the atomization of DF and BD [18].

The composition of BD's fatty acid methyl ester (FAME) determines its dielectric characteristics. Given all of the aforementioned applications and the vast range of feedstocks, determining the electrical permittivity (EP) of BD based on its FAME composition is a scientific contribution to the BD industry.

Technical Editor Jader Barbosa Jr.

✉ Dario Alviso
beto.alviso@gmail.com

[1] Laboratorio de Fluidodinámica, Facultad de Ingeniería, Universidad de Buenos Aires/CONICET, Paseo Colón 850, 1063 Buenos Aires, Argentina

[2] Universidad María Auxiliadora, Mario Halley Mora c/ Palo Santo, Mariano Roque Alonso, Paraguay

Published online: 13 March 2022

Other BD properties have recently been predicted using regression models derived from its FAME content and molecular structure. These properties include the cloud point [19–22], pour point [19–22], flash point [21, 23], cold filter plugging point [20, 21, 23–25], kinematic viscosity [21, 23, 26–29], density [23, 26–28], iodine number [21–23, 29, 30], cetane number [21–23, 26, 28, 31], refractive index, and speed of sound [32, 33].

BD may be produced from hundreds of different VOs [34]. EP experimental values for the majority of these BD have yet to be determined. Regression models of this electrical property that provide an estimate of missing data can be quite useful. There are currently no regression models for BD EP depending on its FAME content and molecular structure. In this article, which may be regarded as a continuation of [21], these regression models are proposed utilizing experimental databases that are provided next.

2 Experimental data

Most materials' dielectric characteristics change dramatically depending on the applied electric field frequency. When an electric field is supplied to a sample, the material's polarization does not change instantly, and a phase difference between the applied electric field signal and the material's polarization is detected. A complex EP is commonly used to depict this phenomenon. The zero-frequency limit of the real portion of the frequency-dependent complex EP is characterized as static EP [33]. The EP is relatively constant (and has its greatest value) at low frequencies when the dipoles have time to follow the applied electric field changes. Then, a sharp decrease of the EP value is observed as the frequency is further increased [7]. Only the values of EP at low frequencies (< 500 kHz) will be used in this study for the regression analysis, considering the frequency range where a constant value of EP is seen.

The real part of the EP (ε_r' in Equation 1) of BD fits a linear equation with the temperature [8].

$$\varepsilon_r'(T) = \varepsilon_r'(T_0) + d\varepsilon_r'/dT(T - T_0) \tag{1}$$

where ε_r' is a non-dimensional quantity, T is the sample temperature in °C, T_0 is the reference temperature in °C, and $d\varepsilon_r'/dT$ is the relative EP temperature coefficient at T_0, in $^\circ C^{-1}$.

Experimental observations performed by multiple authors are required to develop robust regression equations for BD EP. Several investigations with experimental EP values have been published [7, 8, 11, 14, 35, 36]. The publications on BD EP that included both experimental FAME composition values and EP values at frequencies lower than 500 kHz from the literature were selected. In [8] work, the EP values of several BD at 30–50 °C and corresponding FAMEs composition are presented. In [35] work, five pure FAMEs present in most BD were tested at 500 kHz and 20 and 40 °C. Consequently, these works are useful for modeling purposes of the EP regression equations. Unfortunately, in other papers, no information was found concerning the corresponding BD FAME composition. Consequently, only the data presented by [8, 35] will be used to carry out the regression analysis of the BD EP.

Table 1 shows the composition of nine fatty acids as well as the values of the EP in the range of 20–50 °C. Palmitic FAME (C16:0) has 16 carbon atoms and 0 double bonds. Thus, it is a saturated FAME such as stearic, arachidic, and behenic. The remaining FAMEs are unsaturated with one, two, and three double bonds. Palmitic, stearic, oleic, linoleic, and linolenic FAMEs make up the majority of these BD. In addition, EP values drop as temperature rises. Furthermore, the EP values for a particular temperature are relatively close to each other, implying that presenting a regression model with a great agreement to these databases is difficult.

By approximating the experimental results to linear equations, the values of $d\varepsilon_r'/dT$ of Eq. 1 are estimated for each BD and pure FAME. In Table 1, the values of $d\varepsilon_r'/dT$ are of the same order of magnitude. Negative values of $d\varepsilon_r'/dT$ indicate that as the temperature rises, the EP decreases. The regression analysis was carried out at a temperature of $T_0 = 40°C$. This is because the values of each BD and pure FAME are available at this temperature.

3 Results and discussion

3.1 Regression from the FAME composition

Equation 2 shows the BD EP regression equation as a function of FAME content and temperature. The reference temperature T_0 in Eq. 2 is 40 °C, as described in Sect. 2. At this temperature, the regression analysis of EP as a function of FAME composition was carried out. Twelve BD EP measurements at 40 °C were utilized, as shown in Table 1, using values from the [8] and [35] databases. This equation has a constant term, terms based on the mass fractions of saturated and unsaturated FAMEs, and a term that takes into account the EP's temperature dependency. Table 1 provides the appropriate $d\varepsilon_r'/dT$ coefficients for each BD and pure FAME. By using the least-squares approach, these constants and coefficients are calculated. It is worth noting that multiple linear regression (MLR) analysis takes into account regressions that include the nine FAMEs listed in Table 1. Nonetheless, Eq. 2, which only includes the most important BD components, is found to be in good agreement with the experimental results.

Table 1 FAME mass fraction and EP (ε'_r) values of several BD and pure FAMEs extracted from Corach et al. [8] and Gouw and Vlugter [35]. The experimental uncertainty of the EP values in these works is 0.01

	Palmitic	Palmitoleic	Stearic	Oleic	Linoleic	Linolenic	Arachidic	Gadoleic	Behenic	Permittivity						Ref
	C16:0	C16:1	C18:0	C18:1	C18:2	C18:3	C20:0	C20:1	C22:0	20°C	30°C	35°C	40°C	45°C	50°C	$d\varepsilon'_r/dT$	
Olive	0.146	0.0147	0.0216	0.7045	0.0961	0.0047	0.0045	0.0034	0		3.21	3.18	3.15	3.13	3.1	−0.0060	[8]
Canola	0.0383	0.0063	0.0198	0.6736	0.1549	0.0845	0.0062	0.0135	0.0029		3.23	3.21	3.19	3.17	3.14	−0.0044	[8]
Sunflower	0.059	0.0100[a]	0.0398	0.4558	0.4189	0.0025	0.0044	0.0015	0.008		3.25	3.22	3.2	3.17	3.15	−0.0050	[8]
Corn	0.1093	0	0.0264	0.3448	0.4985	0.0079	0.0074	0.0056	0		3.21	3.18	3.16	3.13	3.11	−0.0052	[8]
Soybean	0.1152	0	0.0547	0.2353	0.5119	0.0691	0.0057	0.0041	0.0041		3.19	3.16	3.14	3.12	3.1	−0.0044	[8]
Grape	0.0753	0.0049	0.0508	0.2106	0.6505	0.0031	0.0028	0.0018	0		3.25	3.23	3.2	3.17	3.15	−0.0052	[8]
Chia	0.0674	0.008	0.0337	0.0774	0.1992	0.6095	0.0024	0.0025	0		3.33	3.3	3.28	3.26	3.23	−0.0049	[8]
Palmitic	1	0	0	0	0	0	0	0	0				3.124				[35]
Stearic	0	0	1	0	0	0	0	0	0				3.021				[35]
Oleic	0	0	0	1	0	0	0	0	0	3.211			3.117			−0.0047	[35]
Linoleic	0	0	0	0	1	0	0	0	0	3.355			3.245			−0.0055	[35]
Linolenic	0	0	0	0	0	1	0	0	0	3.466			3.349			−0.0059	[35]

[a]: Myristic fatty acid

$$\varepsilon'_r(T) = 3.121 - \overbrace{0.101x_{ST}}^{saturated} + \overbrace{0.015x_{OL} + 0.110x_{LI} + 0.227x_{LN}}^{unsaturated} + d\varepsilon'_r/dT(T-40) \quad (2)$$

where x_{ST}, x_{OL}, x_{LI}, and x_{LN}, are the mass fraction of stearic, oleic, linoleic, and linolenic FAMEs, respectively.

Experimentally, it has been observed that the EP rises as the carbon chain length and unsaturation increase [7]. Equation 2 accurately reproduces these relationships, since the unsaturated terms tend to increase EP with increasing coefficients, while the saturated term tends to decrease the EP. This regression equation is consequently theoretically sound.

At a reference temperature of 40 °C, Fig. 1 shows the EP experimental data as well as the results of the FAME composition prediction using Eq. 2. Figure 1 shows that the data at 40 °C are distributed for EP values between 3.12 and 3.17 for [8] data and between 3.02 and 3.35 for [35] data, which is consequently wider. The model's statistical coefficients are listed in Table 2. The mean absolute percentage error (MAPE) and root mean square error (RMSE) values for [8] data at 40 °C remain small (0.65 % and 0.026, respectively). The MAPE and RMSE values for [35] data are smaller (0.24 % and 0.011, respectively). Most prediction points lie between the error bands plotted at ±1%. The experimental results are compatible with the dependencies of the BD EP on saturated and unsaturated FAMEs, resulting in satisfactory predicted data.

Figure 2 shows the EP experimental data as well as the results of the FAME composition prediction using Equation 2 at temperatures ranging from 20 to 50 °C. Table 2 also shows the statistical coefficients of the model for each reference and temperature. For data from [8] in the 30–50 °C range, the MAPE (%) and RMSE values remain very similar to those presented at 40 °C, and they are considered very good. For [35] data at 20 °C, even though the agreement is not as good as it was at 40 °C, it is also considered very good, as the MAPE and RMSE values are very small.

3.2 Regression from the molecular structure

In terms of an MLR equation for BD EP as a function of molecular structure, the best agreement to the data in Table 1 was obtained using Equation 3, consisting of a constant term, a term depending on the average number of double bonds n_{db}, and a term that considers the EP's temperature dependence:

$$\varepsilon'_r(T) = 3.058 + 0.091n_{db} + d\varepsilon'_r/dT(T-40) \quad (3)$$

$n_{db} = \sum x_i n_{dbi}$, where n_{dbi} and x_i are, respectively, the number of double bonds and mass fraction of each FAME.

Table 2 Statistical coefficients of the model used to predict the EP of BD from its FAME composition for the data of [8, 35]

Statistics	Corach et al. [8]					Gouw and Vlugter [35]	
	30°C	35°C	40°C	45°C	50°C	20°C	40°C
MAPE (%)	0.62	0.69	0.65	0.68	0.64	0.35	0.24
RMSE	0.024	0.026	0.026	0.026	0.024	0.014	0.011
Nb. of data	7	7	7	7	7	3	5

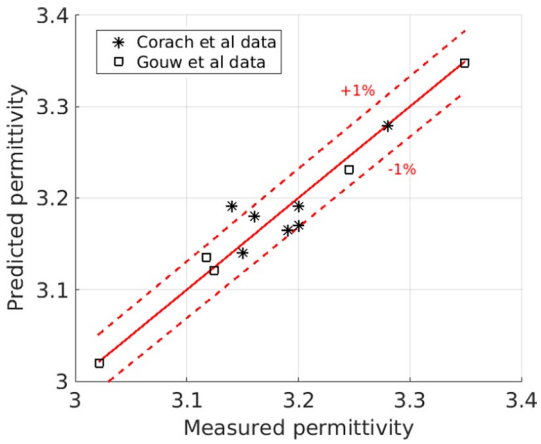

Fig. 1 BD EP experimental data (Corach et al. [8] and Gouw and Vlugter [35]) and prediction from its FAME composition at 40 °C

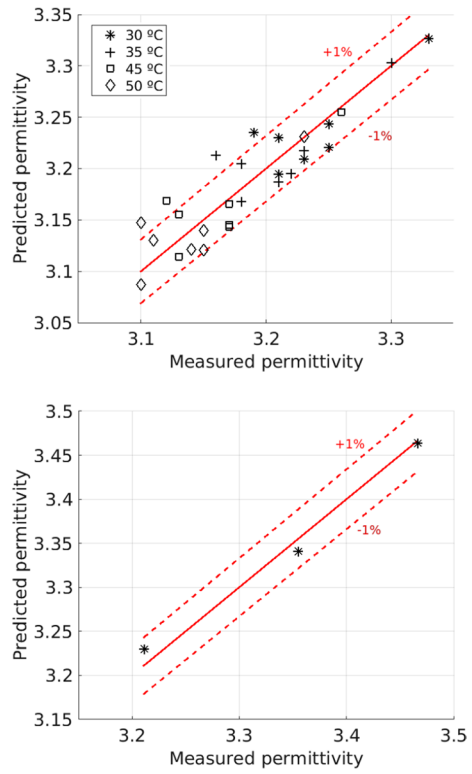

Fig. 2 BD EP experimental data and prediction from its FAME composition at 30–50 °C for Corach et al. [8] on top and at 20 °C for Gouw and Vlugter [35] on bottom

As previously stated, as the unsaturation increases, the EP increases [7]. Equation 3 accurately reproduces this relationship, since the average number of double bonds n_{db} tends to increase the EP. This regression equation is theoretically sound as well.

At 40 °C, Fig. 3 shows the EP experimental data as well as the results of the molecular structure prediction using Eq. 3. The model's statistical coefficients are listed in Table 3. The MAPE (%) and RMSE values for [8] data remain quite small at 40 °C (0.61 % and 0.025, respectively). The MAPE and RMSE values for [35] data are greater this time (1.00 % and 0.038, respectively), but the agreement is still excellent. As the agreement is slightly better, the dependence of the BD EP on the unsaturation level is better reproduced by [8] database.

Figure 4 shows the EP experimental data as well as the results of the molecular structure prediction using Equation 3 at temperatures ranging from 20 to 50 °C. Table 3 also shows the statistical coefficients of the model for each reference and temperature. For data from [8] in the 30–50 °C range, the MAPE (%) and RMSE values remain once again very similar to those presented at 40 °C, and they are considered very good. For [35] data at 20 °C, the agreement is better than it was at 40 °C, as the MAPE and RMSE values are smaller.

4 Conclusions

Even though the EP is not included in BD quality international standards, it has shown to be useful in the study of the BD production process, the quality control of the biofuel and its feedstocks, in the estimation of BD content in its blends with DF, and the estimation of quality properties included in the standards employing correlations.

BD can be produced from hundreds of different VOs. EP values for the majority of these BD have yet to be published. The use of regression equations for this electrical property that allows for the estimate of missing data can be quite useful.

In this article, the EP of BD was calculated using regression models based on its FAME content and molecular structure. The regression analysis was carried out using experimental databases with 43 different data ranging from 20 to

Table 3 Statistical coefficients of the model used to predict the EP of BD from its molecular structure for the data of [8, 35]

	Corach et al. [8]					Gouw and Vlugter [35]	
	30°C	35°C	40°C	45°C	50°C	20°C	40°C
MAPE (%)	0.58	0.62	0.61	0.66	0.59	0.55	1.00
RMSE	0.023	0.025	0.025	0.025	0.023	0.021	0.038
Nb. of data	7	7	7	7	7	3	5

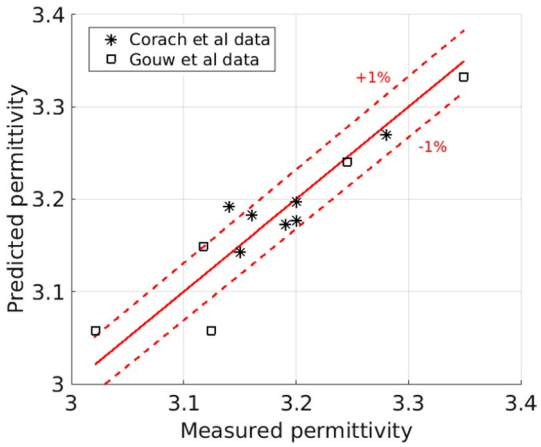

Fig. 3 BD EP experimental data (Corach et al. [8] and Gouw and Vlugter [35]) and prediction from its molecular structure at 40 °C

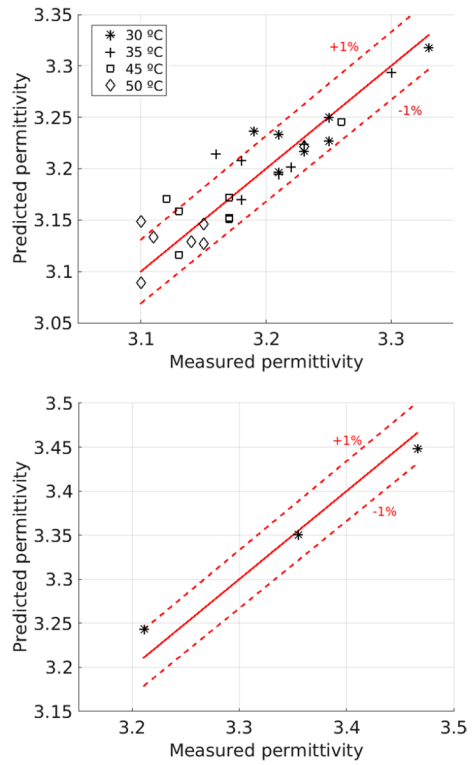

Fig. 4 BD EP experimental data and prediction from its molecular structure at 30–50 °C for Corach et al. [8] on top and at 20 °C for Gouw and Vlugter [35] on bottom

50 °C. MLR analysis was used to obtain the equations. The least-squares approach was used to calculate the constants and coefficients in the equations.

The proposed models for BD EP correctly reproduced its dependence on carbon chain length and unsaturation. The findings from the suggested regression models (based on FAME composition and molecular structure) were compared to the available experimental data, showing a satisfactory agreement. The MAPE and RMSE values were lower than 1% and 0.038, respectively. Finally, both regression models of BD EP derived from its FAME content and molecular structure are in good agreement with the data at various temperatures. Consequently, the equations may be used to estimate EP for oil-based BD for which data are currently unavailable.

Acknowledgements The author would like to thank the Conicet, Argentina, for the financial support.

Declarations

Conflict of interest None.

References

1. Agarwal AK (2007) Biofuels (alcohols and biodiesel) applications as fuels for internal combustion engines. Prog Energy Combust Sci 33(3):233
2. Venkateswarlu K, Murthy B, Subbarao V (2016) An experimental investigation to study the effect of fuel additives and exhaust gas recirculation on combustion and emissions of diesel-biodiesel blends. J Braz Soc Mech Sci Eng 38(3):735
3. Alviso D, Costa MW, Backer L, Pepiot P, Darabiha N, dos Santos RG (2020) Chemical kinetic mechanism for diesel/biodiesel/ethanol surrogates using n-decane/methyl-decanoate/ethanol blends. J Braz Soc Mech Sci Eng 42(2):100
4. Mattos RAD, Bastos FA, Tubino M (2015) Correlation between the composition and flash point of diesel-biodiesel blends. J Braz Chem Soc 26(2):393
5. Júnior LCSS, Ferreira VP, da Silva JA, Torres EA, Pepe IM (2018) Oxidized biodiesel as a cetane improver for diesel-biodiesel-ethanol mixtures in a vehicle engine. J Braz Soc Mech Sci Eng 40(2):79
6. Alviso D, Saab E, Clevenot P, Romano SD (2020) Flash point, kinematic viscosity and refractive index: variations and correlations of biodiesel-diesel blends. J Braz Soc Mech Sci Eng 42(347):347

7. Lizhi H, Toyoda K, Ihara I (2008) Dielectric properties of edible oils and fatty acids as a function of frequency, temperature, moisture and composition. J Food Eng 88(2):151
8. Corach J, Sorichetti PA, Romano SD (2015) Electrical and ultrasonic properties of vegetable oils and biodiesel. Fuel 139:466
9. Cataldo A, Piuzzi E, Cannazza G, De Benedetto E (2012) Classification and adulteration control of vegetable oils based on microwave reflectometry analysis. J Food Eng 112(4):338
10. Lapuerta M, Rodríguez-Fernández J, Patiño-Camino R, Cova-Bonillo A, Monedero E, Meziani YM (2020) Determination of optical and dielectric properties of blends of alcohol with diesel and biodiesel fuels from terahertz spectroscopy. Fuel 274:117877
11. Muley PD, Boldor D (2013) Investigation of microwave dielectric properties of biodiesel components. Bioresour Technol 127:165
12. Corach J, Colman M, Sorichetti PA, Romano SD (2017) Kinematic viscosity of soybean biodiesel and diesel fossil fuel blends: estimation from permittivity and temperature. Fuel 207:488
13. De Souza J, Scherer M, Cáceres J, Caires A, M'Peko JC (2013) A close dielectric spectroscopic analysis of diesel/biodiesel blends and potential dielectric approaches for biodiesel content assessment. Fuel 105:705
14. Diniz Carvalho C, Barros AK, Lopes MV, Silva FC, Santana EE, Sinfrônio FSM (2016) Determination of the composition of biodiesel-diesel blends using the dielectric constant. Instrum Sci Technol 44(4):377
15. Corach J, Sorichetti P, Romano S (2014) Electrical properties of vegetable oils between 20 Hz and 2 MHz. Int J Hydrogen Energy 39(16):8754
16. Eskiner M, Bär F, Rossner M, Munack A, Krahl J (2015) Determining the aging degree of domestic heating oil blended with biodiesel by means of dielectric spectroscopy. Fuel 143:327
17. Cataldo A, Piuzzi E, Cannazza G, De Benedetto E, Tarricone L (2010) Quality and anti-adulteration control of vegetable oils through microwave dielectric spectroscopy. Measurement 43(8):1031
18. Singh G, Pham P, Kourmatzis A, Masri A (2019) Effect of electric charge and temperature on the near-field atomization of diesel and biodiesel. Fuel 241:941
19. Sarin A, Arora R, Singh N, Sarin R, Malhotra R, Kundu K (2009) Effect of blends of Palm-Jatropha-Pongamia biodiesels on cloud point and pour point. Energy 34(11):2016
20. Bolonio D, Llamas A, Rodríguez-Fernández J, Al-Lal AM, Canoira L, Lapuerta M, Gómez L (2015) Estimation of cold flow performance and oxidation stability of fatty acid ethyl esters from lipids obtained from Escherichia coli. Energy Fuels 29(4):2493
21. Alviso D, Artana G, Duriez T (2020) Prediction of biodiesel physico-chemical properties from its fatty acid composition using genetic programming. Fuel 264:116844
22. Alviso D, Zárate C, Duriez T (2021) Modeling of vegetable oils cloud point, pour point, cetane number and iodine number from their composition using genetic programming. Fuel 284:119026
23. Martínez G, Sánchez N, Encinar J, González J (2014) Fuel properties of biodiesel from vegetable oils and oil mixtures. Influence of methyl esters distribution. Biomass Bioenergy 63:22
24. Ramos MJ, Fernández CM, Casas A, Rodríguez L, Pérez Á (2009) Influence of fatty acid composition of raw materials on biodiesel properties. Bioresour Technol 100(1):261
25. Yuan MH, Chen YH, Chen JH, Luo YM (2017) Dependence of cold filter plugging point on saturated fatty acid profile of biodiesel blends derived from different feedstocks. Fuel 195:59
26. Ramírez-Verduzco LF, Rodríguez-Rodríguez JE, del Rayo Jaramillo-Jacob A (2012) Predicting cetane number, kinematic viscosity, density and higher heating value of biodiesel from its fatty acid methyl ester composition. Fuel 91(1):102
27. Verduzco LFR (2013) Density and viscosity of biodiesel as a function of temperature: empirical models. Renew Sustain Energy Rev 19:652
28. Giakoumis EG, Sarakatsanis CK (2018) Estimation of biodiesel cetane number, density, kinematic viscosity and heating values from its fatty acid weight composition. Fuel 222:574
29. Barradas Filho AO, Barros AKD, Labidi S, Viegas IMA, Marques DB, Romariz AR, de Sousa RM, Marques ALB, Marques EP (2015) Application of artificial neural networks to predict viscosity, iodine value and induction period of biodiesel focused on the study of oxidative stability. Fuel 145:127
30. Gopinath A, Puhan S, Nagarajan G (2009) Theoretical modeling of iodine value and saponification value of biodiesel fuels from their fatty acid composition. Renew Energy 34(7):1806
31. Piloto-Rodríguez R, Sánchez-Borroto Y, Lapuerta M, Goyos-Pérez L, Verhelst S (2013) Prediction of the cetane number of biodiesel using artificial neural networks and multiple linear regression. Energy Convers Manag 65:255
32. Alviso D, Romano SD (2021) Prediction of the refractive index and speed of sound of biodiesel from its composition and molecular structure. Fuel 304:120606
33. Alviso D, Zárate C, Artana G, Duriez T (2021) Regressions of the dielectric constant and speed of sound of vegetable oils from their composition and temperature using genetic programming. J Food Compos Anal 104:104175
34. Sajjadi B, Raman AAA, Arandiyan H (2016) A comprehensive review on properties of edible and non-edible vegetable oil-based biodiesel: composition, specifications and prediction models. Renew Sustain Energy Rev 63:62
35. Gouw T, Vlugter J (1964) Physical properties of fatty acid methyl esters. V. Dielectric constant. J Am Oil Chemists' Soc 41(10):675
36. Yeong S, Law M, You K, Chan Y, Lee VC (2019) A coupled electromagnetic-thermal-fluid-kinetic model for microwave-assisted production of Palm Fatty Acid Distillate biodiesel. Appl Energy 237:457